universe

MDPI

Conference Report

Gravitational Waves in Einstein-Æther Theory and Generalized TeVeS Theory after GW170817

Shaoqi Hou † **and Yungui Gong** *

School of Physics, Huazhong University of Science and Technology, Wuhan 430074, China; shou1397@hust.edu.cn

* Correspondence: yggong@hust.edu.cn

† Talk given by this author on the conference of International Conference on Quantum Gravity, SUSTech, Shenzhen, China, 26–28 March 2018.

Received: 27 June 2018; Accepted: 30 July 2018; Published: 1 August 2018

Abstract: In this paper , the polarization contents of Einstein-æther theory and the generalized TeVeS theory are studied. The Einstein-æther theory has five polarizations, while the generalized TeVeS theory has six. In particular, transverse and longitudinal breathing polarization are mixed. The possibility of using pulsar timing arrays to detect the extra polarizations in Einstein-æther theory was also investigated. The analysis showed that different polarizations cannot be easily distinguished by using pulsar timing arrays in this theory. For generalized TeVeS theory, one of the propagating modes travels much faster than the speed of light due to the speed bound set by GW170817. In some parameter subspaces, the strong coupling does not take place, so this theory is excluded.

Keywords: gravitational waves; local Lorentz violation; speed of light

1. Introduction

The Laser Interferometer Gravitational-Wave Observatory (LIGO) Scientific and Virgo collaborations have detected gravitational waves since 14 September 2015 [1–6]. A new era began when it became possible to probe general relativity (GR) through the high speed, strong-field regime. Among the six detections, GW170817 was the first binary neutron star merger event, accompanied by gamma-ray burst GRB 170817A [5,7,8]. Observations led to a very stringent constraint on the speed of GWs , which constrains many alternative theories of gravity. Alternatives to GR usually predict that GWs have up to four additional polarizations in addition to the plus and cross ones [9–15]. Einstein-æther theory [16] and the generalized tensor-vector-scalar (TeVeS) theory [17] contain several extra degrees of freedom (d.o.f.), so it predicts many extra polarizations. The identification of these extra polarizations and their detection are the main topics of this paper . We also take into account the implications of the existing experimental constraints on these theories, especially including the speed bounds from GW170817. A gauge-invariant formalism is devised to obtain GW solutions and identify the polarizations. For a discussion on the GWs of black holes according to Einstein-æther theory, please refer to Refs. [18,19].

In this paper , we first present the GW solutions in Einstein-æther theory in Section 2, where we solve the equations of motion. We thus find the polarization states. Then, we discuss the constraints on the theory, and after that, the possible detection by pulsar timing arrays. A similar analysis is also applied to generalized TeVeS theory in Section 3. Throughout this paper , units are chosen such that the speed of light in vacuum is $c = 1$.

2. Gravitational Waves in Einstein-Æther Theory

In Einstein-æther theory, gravity is mediated by the metric tensor, $g_{\mu\nu}$, and the normalized timelike æther field u^μ. The action can be found in Ref. [20], and there are four parameters, c_i $(i = 1, 2, 3, 4)$, that

measure the coupling between u^μ and $g_{\mu\nu}$. Since u^μ is normalized and timelike, it defines a preferred reference frame everywhere in the spacetime, so it breaks the local Lorentz invariance (LLI). To obtain GW solutions, the metric and the æther field are perturbed such that $g_{\mu\nu} = \eta_{\mu\nu} + h_{\mu\nu}$, $u^\mu = \underline{u}^\mu + v^\mu$ with $\underline{u}^\mu = \delta^\mu_0$. Then, the linearized equations of motion can be solved to get GW solutions which is the method used to get GW solutions based on the generic theory of gravity. A gauge is usually fixed so that the equations of motion take the form of waves. One may also choose to use gauge-invariant variables [21], as in the present paper. The diffeomorphism invariance of the action allows to define the gauge-invariant variables. First, $h_{\mu\nu}$ and v^μ are decomposed in the following way: $v^0 = h_{00}/2 = \phi$, $v^j = \mu^j + \partial^j\omega$, $h_{tt} = 2\phi$, $h_{tj} = \beta_j + \partial_j\gamma$, and $h_{jk} = h^{\rm TT}_{jk} + H\delta_{jk}/3 + \partial_{(j}\epsilon_{k)} + \left(\partial_j\partial_k - \frac{1}{3}\delta_{jk}\nabla^2\right)\rho$ [21]. Here, $h^{\rm TT}_{jk}$ satisfies $\partial^k h^{\rm TT}_{jk} = 0$ and $\eta^{jk}h^{\rm TT}_{jk} = 0$. β_j, ϵ_j and μ^j are transverse vectors. Nine gauge-invariant variables can be constructed, which are $h^{\rm TT}_{jk}$, $\Phi = -\phi + \dot\gamma - \frac{1}{2}\ddot\rho$, $\Theta = \frac{1}{3}(H - \nabla^2\rho)$, $\Omega = \omega + \frac{1}{2}\dot\rho$, $\Xi_j = \beta_j - \frac{1}{2}\dot\epsilon_j$, and $\Sigma_j = \beta_j + \mu_j$ [22]. Not all of them are propagating. In fact, solving the equations of motion gives five propagating d.o.f.: $h^{\rm TT}_{jk}$, Σ_j and Ω. They generally propagate at three different speeds: s_g, s_v, and s_s.

Polarizations of gravitational waves: If the matter fields minimally couple with $g_{\mu\nu}$ only, the polarization content of GWs is determined by the linearized geodesic deviation equation $\ddot{x}^j = d^2x^j/dt^2 = -R_{tjtk}x^k$ with x^j being the deviation vector. Assuming the plane GWs propagate in the $+z$ direction, one can easily identify the polarizations. The plus polarization is given by $\hat{P}_+ = -R_{txtx} + R_{tyty} = \ddot{h}_+$, and the cross polarization is $\hat{P}_\times = R_{txty} = -\ddot{h}_\times$. The vector-$x$ polarization is represented by $\hat{P}_{xz} = R_{txtz} \propto \partial_3\dot\Sigma_1$, and the vector-$y$ polarization is $\hat{P}_{yz} = R_{txty} \propto \partial_3\dot\Sigma_2$. The transverse breathing polarization is specified by $\hat{P}_b = R_{txtx} + R_{tyty} \propto \ddot\Omega$, and the longitudinal polarization is $\hat{P}_l = R_{tztz} \propto \ddot\Omega$. Note that Ω excites a mixed state of $\hat{P}_b$ and $\hat{P}_l$.

Discussion on the constraints: Previous observations have set various constraints on the parameter space of the theory. These constraints include these on the post-Newtonian parameters, α_1 and α_2 [12], and the requirements that the GW carry positive energy [23], and there should not be gravitational Cherenkov radiation [24] etc. Combining all the constraints shows that this theory is highly constrained. To make more explicit predictions, we picked some specific points in the allowed parameter space, as shown in Table 1. In the left table, c_is take values such that LLI is respected, while in the right table, LLI is violated. It is clear that these values are very small which requires severe fine-tuning.

Table 1. The choices of parameters and the corresponding speeds of the vector and scalar GWs. In the left part of the table, c_is are normalized by 10^{-16} and $s_g = 1 + 7\times10^{-15}$. In the right part of the table, c_is are normalized by 10^{-9} and $s_g = 1$.

c_1	7.7	8.4	9.1	$c_1 = -c_3$	6.06	3.59	2.83
c_2	−5.5	−6.2	−6.8	c_2	3.66	2.58	2.10
c_3	6.3	5.6	4.9	c_4	−4.06	−1.59	−0.83
c_4	−5.2	−3.7	−2.6				
s_v	1.74	1.34	1.19	s_v	1.74	1.34	1.19
s_s	1.83	1.29	1.05	s_s	1.83	1.29	1.05

Pulsar timing arrays: Pulsar timing arrays (PTAs) can measure the timing residuals $R(t)$ of photons emitted from pulsars. There is cross correlation between timing residuals for pulsars, which is given by $C(\theta) = \langle R_a(t)R_b(t)\rangle$, where θ is the angular separation between pulsars a and b, and the brackets $\langle\,\rangle$ imply the ensemble average over the stochastic GW background. The functional form of $C(\theta)$ is determined by the type of the polarization of GWs, so PTAs can examine the polarizations of GWs. For Einstein-æther theory, one can calculate $C(\theta)$, and the results are shown in Figures 1 and 2. Figure 1 shows the behavior of $\zeta(\theta) = C(\theta)/C(0)$ as a function of θ for the scalar and the vector polarizations at different speeds corresponding to the values of c_i listed in the left table in Table 1. The GR's prediction (the red solid curves) is also plotted which approximately represents $\zeta(\theta)$ for the tensor GW.

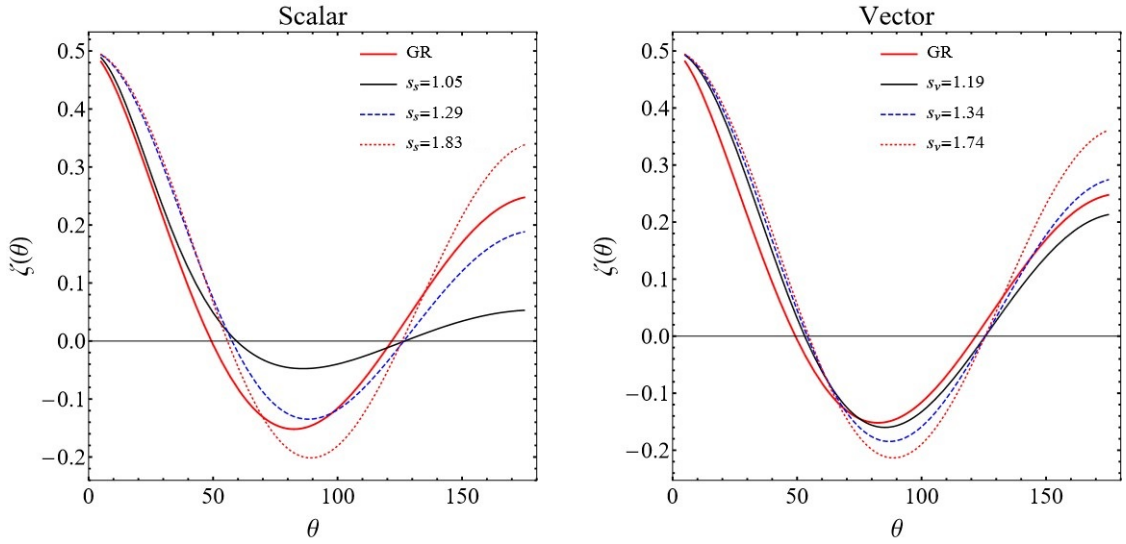

Figure 1. The normalized cross correlation function $\zeta(\theta)$ for the scalar (the **left** panel) and the vector (the **right** panel) GWs when c_i have the values shown in the left table in Table 1.

It is clear that these curves are very similar to each other, so it would be difficult to distinguish different polarizations. If one chooses the values for the c_is given in Table 1, the $\zeta(\theta)$ for the scalar GW is modified, as shown in Figure 2. Since if $c_{13} = 0$, there are no vector polarizations, the corresponding $\zeta(\theta)$ was not plotted. Figure 2 shows that $\zeta(\theta)$ for the scalar GW is very different from the one for the tensor GW. So, it is easier to distinguish the scalar polarizations from the tensor ones.

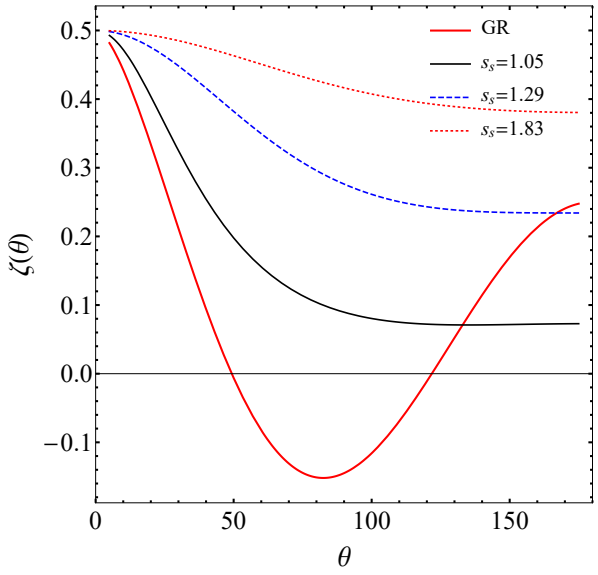

Figure 2. The normalized cross-correlation function $\zeta(\theta) = C_s(\theta)/C_s(0)$ for the scalar GW when the c_is take the values shown in Table 1.

3. Gravitational Waves in the Generalized TeVeS Theory

Generalized TeVeS theory is the generalization of the theory originally proposed by Bekenstein to attack the dark matter problem [25]. Compared with Einstein-æther theory, it has an additional scalar field, σ, which also mediates gravity. Matter fields minimally couple to the physical metric $\tilde{g}_{\mu\nu} = e^{-2\sigma} g_{\mu\nu} - 2u_\mu u_\nu \sinh(2\sigma)$. One can easily verify that there are six d.o.f.: $h^{\rm TT}_{jk}$, Σ_j, Ω, and σ. They propagate at four different speeds named $\tilde{s}_g$, $\tilde{s}_v$, $\tilde{s}_s$ and $\tilde{s}_0$, respectively. In addition, there are

the plus, cross, vector-x, and vector-y polarizations. The two scalar d.o.f. excite two copies of mixed states of the transverse breathing and the longitudinal polarizations. There are also several previous experimental constraints on this theory, as given in Refs. [25–29]. Combining all of these constraints shows that the speed ($\tilde{s}_s$) for Ω is generally much larger than 1, which might lead to the faster decay of binary systems, so this theory might be excluded. However, a very large speed might result in strong coupling. We examined whether strong coupling for Ω takes place. Figure 3 displays the parameter subspaces that are compatible with the experimental constraints. Strong coupling does not exist in the red regions, while in the blue areas, strong coupling takes place. Then, the generalized TeVeS theory is excluded in the parameter space where strong coupling does not exist. Further analysis is required to determine whether it survives in the blue regions.

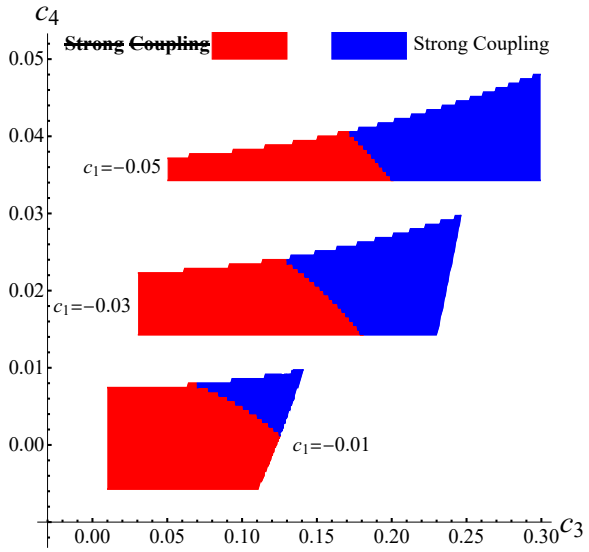

Figure 3. Parameter subspaces (colored areas) allowed by the experimental constraints.

4. Conclusions

In this paper , we used the gauge-invariant variable formalism to obtain the linear GW solutions about the Minkowski background and the polarization contents of Einstein-æther theory and the generalized TeVeS theory. There are five polarization states in Einstein-æther theory and six in generalized TeVeS theory. The longitudinal and transverse breathing modes together form a single state for the scalar d.o.f. in both theories. For Einstein-æther theory, the analysis showed that it might be difficult for PTAs to distinguish different polarizations when LLI is respected, while it is easier to do so when $s_g = 1$ and LLI is violated. For generalized TeVeS theory, it was found out that it is excluded by the speed bounds on GWs in the parameter regions where the strong coupling of the scalar d.o.f. Ω does not suffer from strong coupling.

Author Contributions: Conceptualization, S.H. and Y.G.; Methodology, S.H. and Y.G.; Validation, S.H. and Y.G.; Formal Analysis, S.H.; Investigation, S.H. and Y.G.; Writing—Original Draft Preparation, S.H.; Writing—Review & Editing, S.H. and Y.G.; Visualization, S.H.; Funding Acquisition, Y.G.

Funding: This research was supported, in part, by the Major Program of the National Natural Science Foundation of China under Grant No. 11690021 and the National Natural Science Foundation of China under Grant No. 11475065.

Acknowledgments: We thank Ted Jacobson for constructive discussions. We also thank Cosimo Bambi for the organization of the conference International Conference on Quantum Gravity that took place in Shenzhen, China, 26–28 March 2018. This paper is based on a talk given at the mentioned conference.

Conflicts of Interest: The authors declare no conflict of interest.

References

1. Abbott, B.P.; et al. [LIGO Scientific Collaboration and Virgo Collaboration]. Observation of Gravitational Waves from a Binary Black Hole Merger. *Phys. Rev. Lett.* **2016**, *116*, 061102. [CrossRef] [PubMed]
2. Abbott, B.P.; et al. [LIGO Scientific Collaboration and Virgo Collaboration]. GW151226: Observation of Gravitational Waves from a 22-Solar-Mass Binary Black Hole Coalescence. *Phys. Rev. Lett.* **2016**, *116*, 241103. [CrossRef] [PubMed]
3. Abbott, B.P.; et al. [LIGO Scientific and Virgo Collaboration]. GW170104: Observation of a 50-Solar-Mass Binary Black Hole Coalescence at Redshift 0.2. *Phys. Rev. Lett.* **2017**, *118*, 221101. [CrossRef] [PubMed]
4. Abbott, B.P.; et al. [LIGO Scientific Collaboration and Virgo Collaboration]. GW170814: A Three-Detector Observation of Gravitational Waves from a Binary Black Hole Coalescence. *Phys. Rev. Lett.* **2017**, *119*, 141101. [CrossRef] [PubMed]
5. Abbott, B.P.; et al. [LIGO Scientific Collaboration and Virgo Collaboration]. GW170817: Observation of Gravitational Waves from a Binary Neutron Star Inspiral. *Phys. Rev. Lett.* **2017**, *119*, 161101. [CrossRef] [PubMed]
6. Abbott, B.P.; et al. [LIGO Scientific Collaboration and Virgo Collaboration]. GW170608: Observation of a 19-solar-mass Binary Black Hole Coalescence. *Astrophys. J.* **2017**, *851*, L35. [CrossRef]
7. Goldstein, A.; Veres, P.; Burns, E.; Briggs, M.S.; Hamburg, R.; Kocevski, D.; Wilson-Hodge, C.A.; Preece, R.D.; Poolakkil, S.; Roberts, O.J.; et al. An Ordinary Short Gamma-Ray Burst with Extraordinary Implications: Fermi-GBM Detection of GRB 170817A. *Astrophys. J.* **2017**, *848*, L14. [CrossRef]
8. Savchenko, V.; Ferrigno, C.; Kuulkers, E.; Bazzano, A.; Bozzo, E.; Brandt, S.; Chenevez, J.; Courvoisier, T.L.; Diehl, R.; Domingo, A.; et al. INTEGRAL Detection of the First Prompt Gamma-Ray Signal Coincident with the Gravitational-wave Event GW170817. *Astrophys. J.* **2017**, *848*, L15. [CrossRef]
9. Eardley, D.M.; Lee, D.L.; Lightman, A.P. Gravitational-wave observations as a tool for testing relativistic gravity. *Phys. Rev. D* **1973**, *8*, 3308–3321. [CrossRef]
10. Capozziello, S.; De Laurentis, M.; Luongo, O.; Ruggeri, A. Cosmographic Constraints and Cosmic Fluids. *Galaxies* **2013**, *1*, 216–260. [CrossRef]
11. Capozziello, S.; De Laurentis, M.; Luongo, O. Connecting early and late universe by $f(R)$ gravity. *Int. J. Mod. Phys. D* **2014**, *24*, 1541002. [CrossRef]
12. Will, C.M. The Confrontation between General Relativity and Experiment. *Living Rev. Rel.* **2014**, *17*, 4. [CrossRef] [PubMed]
13. Liang, D.; Gong, Y.; Hou, S.; Liu, Y. Polarizations of gravitational waves in $f(R)$ gravity. *Phys. Rev. D* **2017**, *95*, 104034. [CrossRef]
14. Hou, S.; Gong, Y.; Liu, Y. Polarizations of Gravitational Waves in Horndeski Theory. *Eur. Phys. J. C* **2018**, *78*, 378. [CrossRef]
15. Gong, Y.; Hou, S. Gravitational Wave Polarizations in $f(R)$ Gravity and Scalar-Tensor Theory. In Proceedings of the 13th International Conference on Gravitation, Astrophysics and Cosmology and 15th Italian-Korean Symposium on Relativistic Astrophysics (IK15), Seoul, Korea, 3–7 July 2017; Volume 168, p. 01003.
16. Jacobson, T.; Mattingly, D. Gravity with a dynamical preferred frame. *Phys. Rev. D* **2001**, *64*, 024028. [CrossRef]
17. Seifert, M.D. Stability of spherically symmetric solutions in modified theories of gravity. *Phys. Rev. D* **2007**, *76*, 064002. [CrossRef]
18. Konoplya, R.A.; Zhidenko, A. Gravitational spectrum of black holes in the Einstein-Aether theory. *Phys. Lett. B* **2007**, *648*, 236–239. [CrossRef]
19. Konoplya, R.A.; Zhidenko, A. Perturbations and quasi-normal modes of black holes in Einstein-Aether theory. *Phys. Lett. B* **2007**, *644*, 186–191. [CrossRef]
20. Jacobson, T.; Mattingly, D. Einstein-Aether waves. *Phys. Rev. D* **2004**, *70*, 024003. [CrossRef]
21. Flanagan, E.E.; Hughes, S.A. The Basics of gravitational wave theory. *New J. Phys.* **2005**, *7*, 204. [CrossRef]
22. Gong, Y.; Hou, S.; Liang, D.; Papantonopoulos, E. Gravitational waves in Einstein-æther and generalized TeVeS theory after GW170817. *Phys. Rev. D* **2018**, *97*, 084040. [CrossRef]
23. Jacobson, T. Einstein-aether gravity: A Status report. In Proceedings of the From Quantum to Emergent Gravity: Theory and Phenomenology, Trieste, Italy, 11–15 June 2007.

24. Elliott, J.W.; Moore, G.D.; Stoica, H. Constraining the new Aether: Gravitational Cerenkov radiation. *J. High Energy Phys.* **2005**, *2005*, 066. [CrossRef]
25. Bekenstein, J.D. Relativistic gravitation theory for the MOND paradigm. *Phys. Rev. D* **2004**, *70*, 083509. [CrossRef]
26. Sagi, E. Preferred frame parameters in the tensor-vector-scalar theory of gravity and its generalization. *Phys. Rev. D* **2009**, *80*, 044032. [CrossRef]
27. Sagi, E.; Bekenstein, J.D. Black holes in the TeVeS theory of gravity and their thermodynamics. *Phys. Rev. D* **2008**, *77*, 024010. [CrossRef]
28. Lasky, P.D.; Sotani, H.; Giannios, D. Structure of Neutron Stars in Tensor-Vector-Scalar Theory. *Phys. Rev. D* **2008**, *78*, 104019. [CrossRef]
29. Lasky, P.D. Black holes and neutron stars in the generalized tensor-vector-scalar theory. *Phys. Rev. D* **2009**, *80*, 081501. [CrossRef]